HELICOPTER PARAMETERS ESTIMATION FROM SUBSPACE IDENTIFICATION BY CONSTRAINED NONLINEAR OPTIMIZATION

Sevil Avcıoğlu, Turkish Aerospace Industries, savcioglu@tai.com.tr
Ali Türker Kutay, Middle East Technical University, Aerospace Eng.
Kemal Leblebicioğlu, Middle East Technical University, Elect. and Electronics Eng.
Yakup Özkazanç, Hacettepe University, Elect. and Electronics Eng.
İlkay Yavrucuk, Middle East Technical University, Aerospace Eng.
Ankara, Turkey

Abstract

Subspace identification uses well-understood techniques based on linear algebra and numerical methods. However, the state space model matrices which are obtained from conventional subspace identification algorithms are not necessarily associated with the physical states. This may be evaluated as a deficiency for the area of helicopter flight dynamics where physical parameter estimation is mainly conducted for mathematical model improvement, aerodynamic parameter validation and flight controller tuning. There are a limited number of studies in literature, which tackle this problem. Some of these studies are based on nonlinear optimization. However this optimization problem may have infinitely many solutions if we do not define well-founded constraints. It may be possible to estimate the real physical parameters by establishing the constraints which compatible with practical values. This study focuses on to the determination physical constraints for the parameters which are confined to the problem described here. For this purpose, the subjected parameters are examined according to their physical meaning. Both the expected theoretical values and the experimental knowledge are evaluated to determine the constraints. Then, many runs are conducted for these predefined constraints with randomly selected initial conditions.

1. NOMENCLATURE

N4SID	: “Numerical Algorithms for Subspace State Space System Identification”
MOESP	:“Multivariable Output-Error State Space”.
u, v, w	:translational velocity components (longitudinal, lateral, vertical), ft/s
p, q, r	:angular velocity components (roll, pitch, yaw), deg/s
ϕ, θ	: Euler angles (roll, pitch), deg
A, B, C, D	:state space matrices found by subspace identification
$A_{phy}, B_{phy}, \dots$	:state space matrices found by physical subspace identification
$X_u, X_v, X_w, \dots$	:force to translational velocity derivatives, $1/s$
$X_p, X_q, X_r, \dots$	:force to angular velocity derivatives, $ft/(deg.s)$
$L_u, L_v, L_w, \dots$	:moment to translational velocity derivatives, $deg/(ft \cdot s)$
$L_p, L_q, L_r, \dots$	:moment to angular velocity derivatives, $1/s$
$X_{\delta_{lat}}, X_{\delta_{lon}}$.	:force to control input derivatives, $ft/(s^2 \cdot \%)$
$L_{\delta_{lat}}, L_{\delta_{lon}}, ..$	:force to control input derivatives, $deg/(s^2 \cdot \%)$
g	:gravity force, ft/s^2
ρ	:air density, $slug/ft$^3
a_0	:main rotor lift curve slope, $1/rad$
μ	:advance ratio
Ω	:main rotor speed
R	:main rotor radius, ft
A_b	:blade area, ft^2
M_a	:mass of helicopter, lb
s	:rotor solidity
NA	:Not Applicable

2. INTRODUCTION

The interest of helicopter design society on subspace identification methods arise in the last decade [1]. Until now, some variants of subspace identification algorithms like N4SID and MOESP ([1] – [10]) were applied on a number of

Presented at 45th European Rotorcraft Forum, Warsaw, Poland, 17-20 September, 2019

helicopters by using simulation or flight test data. However, the state space model matrices which are obtained from conventional subspace identification algorithms are not necessarily associated with the physical parameters [1]. Physical parameter estimation based on subspace identification for helicopter systems is still being investigated. There exist studies on this problem in the area of helicopter flight dynamics ([11] – [13]). These studies utilize Laguerre filters to convert the discrete time state space models into continuous models. Another approach for finding the physical parameters from subspace identification results is optimization. Similarity transformation of a discrete LTI system $\bar{x} = T^{-1}x$ which leads to a new set of state space matrices is used for this purpose (Eq (1)-(3)).

(1) $$\bar{A} = T^{-1}AT$$

(2) $$\bar{B} = T^{-1}B$$

(3) $$\bar{C} = CT$$

The aim is to find the $\bar{\mathrm{A}}, \bar{\mathrm{B}}, \bar{\mathrm{C}}$ matrices with the similarity transformation matrix T which lead us to the physical parameters. The objective function is defined as the sum squares of the difference between the right and left side of the similarity transformation equations Eq. (1)-(3) where the equality and the inequality constraints are determined with physical insight.

There are a limited number of studies in the literature which tackle with this problem ([14]-[19]). These studies propose basic methodologies like least square or quadratic optimization and most of them are applied for relatively simple systems. Helicopter identification requires far more variables to be solved. Therefore it may require more advanced optimization algorithms. The preliminary study is tackled in [20] to estimate the helicopter physical parameters from subspace identification. In [20], it is assumed that all of the stability and control derivatives are known with ±20% error. The initial values of these parameters are selected as randomly. The aim of this study to enhance the methodology given [20] by setting the constraints with more specifically selected values. For this purpose, the constraints for the stability and control derivatives are chosen regarding the well-known dynamics and the measurable properties of the helicopter.

3. SUBSPACE IDENTIFICATION

For a given input output data set, subspace identification can find the state space matrices A, B, C, D and the hidden states x even if the dimensions of x is unknown. Out of many available subspace identification methods in the literature ([1]–[4]), the "Robust Subspace Algorithm" which proved itself in many industrial applications ([1] Chapter 4, Algorithm 3) is selected in this study. "Robust Subspace Algorithm" begins with the calculation of the oblique projection as given in Eq. (4).

(4) $$O_i = Y_f /_{U_f} W_p$$

Y_f is the Block Hankel matrices of the future outputs. U_f is Block Hankel matrices of the future inputs. W_p is the Block Hankel matrices of past inputs and outputs. This operation projects Y_f along the row space of U_f on the row space of W_p.

Singular Value Decomposition (SVD) of O_i is performed for model order reduction (Eq.(5)).

(5) $$O_i = USV^T = US^{1/2}S^{1/2}V^T$$

O_i, which is now represented in the SVD form, can also be represented by the product of the extended observability matrix, Γ_i and the state sequence matrix, X_i. The proof of this is given in [1]

(6) $$O_i = \Gamma_i X_i$$

Another projection matrix is the prediction matrix, Z_i. The prediction matrix, Z_i is considered as an optimal prediction of the future output, Y_f on the subspace formed by Block Hankel matrices of past inputs and outputs, W_p and the Block Hankel matrices of the future input, U_f. The corresponding formulation is shown in Eq. (7).

(7) $$Z_i = Y_f / \begin{pmatrix} W_p \\ U_f \end{pmatrix}$$

We have now defined all of the matrices required to calculate the system matrices A and C according to the theory. System matrices A and C can now be calculated from Eq. (8) using the least square approach (The related derivations are given in [1] Chapter 4).

(8) $$\begin{pmatrix} \Gamma_{i-1}^{\dagger} Z_{i+1} \\ Y_{i|i} \end{pmatrix} = \begin{pmatrix} A \\ C \end{pmatrix} \Gamma_i^{\dagger} Z_i + \kappa U_f + \begin{matrix} \rho_w \\ \rho_v \end{matrix}$$

where the intermediate matrix, κ and the lower block triangular Toeplitz matrix, H_i are given in [1]. Here ρ_w,ρ_v are the covariances of the process and measurement noise of the residuals.

Then the remaining system matrices B and D are

Presented at 45th European Rotorcraft Forum, Warsaw, Poland, 17-20 September, 2019

calculated by solving the minimization problem shown in Eq. (9). The intermediate steps are explained in [1], Chapter 4 in more detail.

(9) B, D

$$= arg\,min_{B,D} \left\| \begin{pmatrix} \Gamma_{i-1}^{\dagger} Z_{i+1} \\ Y_{(i|i)} \end{pmatrix} - \begin{pmatrix} A \\ C \end{pmatrix} \Gamma_i^{\dagger} Z_i - \kappa(B,D) U_f \right\|_F$$

The system matrices A, B, C, D found through the above given formulation do not necessarily have a direct physical interpretation but they have a conceptual relevance, [1]. According to the similarity transformation theory [21], the state vector of a discrete LTI system can be transformed into another state vector. This is shown in Eq. (10).

(10) $$x_{phy} = T^{-1} x$$

Such an operation leads to a new set of state space matrices as shown in Eq. (11)-(13)

(11) $$A_{phy} = T^{-1} A T$$

(12) $$B_{phy} = T^{-1} B$$

(13) $$C_{phy} = C T$$

This will hopefully lead us to the physical parameters which take part in A_{phy}, B_{phy} and C_{phy} matrices the with the corresponding similarity transformation matrix, T. Since both the physical system matrices and the similarity transformation matrix is lacking, a candidate solution is the minimization of the difference between the left hand side and the right hand side of Eq.(11)-(13). This can be achieved by an optimization that makes use of the lower bound of the sum squares of the difference between the right and left sides [17]–[19]. In order to reduce the nonlinearity of the problem we rewrite the equations as in Eq.(14) and Eq.(15), [17].

(14) $$T A_{phy} = A T$$

(15) $$T B_{phy} = B$$

4. MODEL STRUCTURE

The model structure of an aerospace vehicle is usually obtained from the governing 6-DOF flight-dynamics equations. These equations inherently contain a substantial amount of parameters required for validating mathematical models, wind tunnel test results and for tuning the flight controller gains.

The state space model structure derived for the 6-DOF nonlinear equations of motion for a helicopter [22] can be written as in Appendix. The force derivatives are normalized by mass, and the moment derivatives are normalized by the corresponding moments of inertia. Moreover for the moment derivatives, a pre-multiplication by the inertia tensor has been carried out so that they implicitly include products of inertia terms (i.e. I_{xy}, I_{xz}, etc.), [22]. The proposed model structure has 8 states and 4 inputs. These are given in Eq.(16)-Eq.(18) respectively.

(16) $$\dot{x}_{phy} = A_{phy} x_{phy} + B_{phy} u$$

(17) $$x_{phy} = [\, u\ v\ w\ p\ q\ r\ \phi\ \theta\,]$$

(18) $$u = [\, \delta_{lat}\ \delta_{lon}\ \delta_{ped}\ \delta_{col}\,]$$

When the rest of the state space matrices are concerned, with the assumption that all of the system states are perfectly measurable, the associated C_{phy} is an identity matrix and according to our problem formulation D_{phy} is equal to zero.

Since all of the states are assumed to be perfectly measurable, the total number of parameters to be estimated in the A_{phy}, B_{phy} and T matrices are 36, 24 and 64 respectively. Therefore altogether there are 124 unknowns. Such a problem can be classified as an optimization problem with large number of variables. The solution methodology is explained in the following paragraph.

5. PARAMETER ESTIMATION

Consider an optimization problem;

(19) $$\begin{aligned} &minimize && minf(\chi) \\ &subject\ to && \chi \in \Omega \end{aligned}$$

The real-valued function $f: \mathbb{R}^n \longrightarrow \mathbb{R}$ which is desired to be minimized is named as an objective function. The vector χ is an vector with *n* independent variables:$\chi = [x_1,\ x_2, x_3, \dots, x_n]^T \in \mathbb{R}^n$. The set Ω is a subset of $\mathbb{R}^n$ called the constraint set or feasible set. In our problem, the objective function shown in Eq. (20) is the sum squares of the difference between the right and left side of the similarity transformation equations Eq. (13), Eq.(14), and Eq. (15), [17] – [19].

(20) $$\begin{aligned} &\min_{\chi} f(\chi) \\ &= \min_{\chi} \Big(\left\| T(\chi) A_{phy}(\chi) - A T(\chi) \right\|_F \\ &\qquad + \left\| T(\chi) B_{phy}(\chi) - B \right\|_F \\ &\qquad + \left\| C_{phy}(\chi) - C T(\chi) \right\|_F \Big) \end{aligned}$$

Due to the nonlinear characteristics of the objective function, this problem can be handled by

Presented at 45th European Rotorcraft Forum, Warsaw, Poland, 17-20 September, 2019

NonLinear Programming (NLP), [14]–[16]. In the literature, there exist a number of algorithms for solving NLP problems. In our case, we decided to concentrate on "large-scale" NLP algorithms where the total number of variables is greater than one hundred. In this problem we selected the Sequential Quadratic Programming (SQP) which is well-known algorithm for large scale problems.

6. CONSTRAINT SELECTION

From infinitely many state space model, it may be possible to find a solution set which consists of physical parameters. One way to estimate physical model is constraint selection. Defining a proper constraint values may ensure as to estimate the physical parameters. For this purpose, following subjects are examined to determine the constraints.

6.1. "insignificant" derivatives

As it is mentioned above, there exists 60 parameters to be estimated (36 parameters in A_{phy} and 24 parameters in B_{phy}) in our problem. However, they are not all the same in the sense of significance. Some of them are quite insignificant compare to the others. In this study, the insignificant parameters are set to zero as it is common practice. In fact, these "insignificant" parameters vary from helicopter to helicopter due to their dynamic characteristics. Flight region is another condition which affects the elements of the "insignificant" parameters set. For common practice, the stability parameters $X_v, X_w, Y_u, Y_w, Z_u,$ Z_v, M_v, M_r, N_w and the control parameters $X_{\delta_{ped}}$, $Y_{\delta_{ped}}, M_{\delta_{ped}}, Y_{\delta_{col}}$ are assumed as "insignificant". Therefore these parameters are set to zero.

Considering the high forward velocity flight conditions where the inertial velocities are so dominant, the aerodynamic effects may be negligible (e.g., Z_q , Y_r), [22].

6.2. Stability derivatives

Some parameters implicate powerful information about the helicopter stability. These derivatives are tabulated in Table 1 with the expected values regarding stability, [22].

Table 1 Derivatives with Expected Values to Ensure Stability

Stability Criteria	Expected Value
Dihedral effect	$L_v < 0$
Roll damping	$L_p < 0$
Yaw to roll coupling	$L_r > 0$
Static speed stability	$M_u > 0$
Incidence stability	$M_w < 0$
Pitch damping	$M_q < 0$
Weathercock stability	$N_v > 0$
Adverse yaw	$N_p < 0$
Yaw damping	$N_r < 0$
Drag damping	$X_u < 0$
Side Force Damping	$Y_v < 0$
Heave Damping	$Z_w < 0$

Prior stability knowledge about the helicopter which is under examination may give some hint about the sing of these derivatives.

6.3. "Quantifiable" derivatives

Some derivatives can be formulated in terms of quantifiable parameters. For example, approximation for heave damping derivative can be written as in Eq. (18) for forward flight condition, [22].

$$Z_w = -\frac{\rho a_0 \mu (\Omega R) A_b}{2M_a}\left(\frac{4}{8\mu + a_0 s}\right) \tag{21}$$

The derivative of thrust with main rotor collective ($Z_{\delta_{col}}$) and longitudinal cyclic ($Z_{\delta_{lon}}$) which can be obtained from the thrust and uniform inflow equations can be formulated as in Eq. (22) and in Eq. (23), [22].

$$Z_{\delta_{col}} = -\frac{4}{3}\frac{a_0 A_b \rho (\Omega R)^2 \mu (1+\mu^2)}{(8\mu + a_0 s) M_a} \tag{22}$$

$$Z_{\delta_{lon}} = -2\frac{a_0 A_b \rho (\Omega R)^2 \mu^2}{(8\mu + a_0 s) M_a} \tag{23}$$

7. IMPLEMENTATION

The method described on the previous sections, is implemented to flight simulation data. For this purpose we used a nonlinear model of multi role combat helicopter which was developed in FLIGHTLAB. The main rotor has a fully articulated model which includes the associated aerodynamic database, structural dynamics, induced velocity and interference effects. Tail rotor module uses "Actuator Disk Model". Airframe model is comprised of fuselage, horizontal tail and vertical tail components. All of the associated aerodynamic data belongs to wind tunnel test results and numerical analysis performed in FLUENT environment. The flight stability augmentation system model is embedded in the flight control module. Rate feedback stabilization systems for roll, pitch and yaw channels are enabled to increase system stability. These stabilization systems also include the main rotor

Presented at 45th European Rotorcraft Forum, Warsaw, Poland, 17-20 September, 2019

and tail rotor actuator models. Actuator models are linear.

The nonlinear model of multi role combat helicopter is linearized around a specific trim point (level flight at 70 knots, 2000 ft MSL). Linearization is performed by using the linearization feature of FLIGHTLAB. In this process, inputs are selected as lateral cyclic, longitudinal cyclic, pedal and collective; states are selected as translational velocity components (longitudinal, lateral and vertical velocity), angular velocity components (roll, pitch and yaw rates), roll angle and pitch angle; the outputs are assigned to the states. The obtained linear model is transferred to MATLAB environment to utilize for the rest of the analysis.

Now we shall proceed by generating input and output data required for identification. One of the most optimal input signal types which meet the well-known requirement of *persistently exciting* [8], [25] is 3-2-1-1. This input sequence is sequentially applied for each channel during the same identification test. Signal to noise ratio is taken into account while selecting the amplitudes of the input signals. Moreover, helicopter is not allowed to drift away from the trim condition too much [25]. For this purpose input signal amplitudes are limited in such a way that the helicopter attitude angles stay in the range of ± 10 deg around the specific trim point and the helicopter angular velocity components shall not exceed ± 10 deg/s. These considerations about the input design are expected to ensure the quality of identification. Constructed signals for each input channel are shown in Fig. 1. These inputs are fed to the linear model in MATLAB environment to generate the outputs required for identification. The corresponding outputs are presented in Fig. 2.

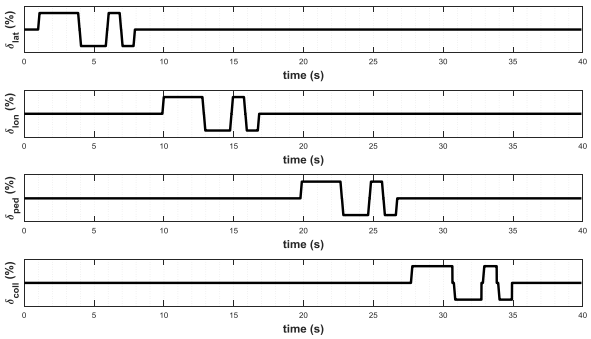

Fig. 1 Input Signals (3-2-1-1)

Since we have an input and output set, we can initiate the identification process. The “Robust Subspace Algorithm” ([1], Chapter 4, Algorithm 3) is utilized to estimate the system matrices in state space form. These matrices which are represented in discrete time linear model are then converted into their continuous time counterparts using “d2c” command of MATLAB. This operation is required since we are seeking for the continuous time form of the system model in order to access to the physical parameters. According to the similarity transformation theory (Eq.(13)-(15)), the objective function presented in Eq. (20) is symbolically generated for our problem. MATLAB symbolic toolbox is used for this purpose.

There are infinitely many numbers of solutions for this minimization problem. However, our aim is to reach to a solution that corresponds to the physical domain. In this study, we propose two complementary approaches about constraint determination. In the first step, the constraints are established by referencing the true model data. As in [20], the constraints are selected considering linearized outputs of FLIGHTLAB with suitable error margins ([-20% 20%]). These error margins are expanded to [-50% 50%] in this study. Then, as a second step, the constraints are reshaped according to physical content of the relevant parameters. For instance, if we have a priori information about the stability characteristics then we can estimate the sign of the stability characteristics more or less. More specifically, if we have an idea about the pitch damping characteristics of the system for predefined flight condition, we can set a sign constraint for the relevant derivative (M_q). All of the stability related parameters which are listed in Table 1 are bounded due to stability characteristics of our system which is under examination. Then, we eliminate the insignificant parameters which are already mentioned in paragraph 6. In addition to all these, the constraints for some derivatives (Z_w, $Z_{\delta_{col}}$ and $Z_{\delta_{lon}}$) are set by calculating the approximations equations (Eq.(18)-(20)) for this study. The constraints for all of the stability and control derivatives defined in the first step are combined with the constraint values for the ones specified in the second step. The final constraints are set to a confined space which is acquired by intersecting of these values.

The initial values are randomly selected between the constraints. In order to assure that the solution is consistent, the optimizations are repeated for many times of randomly selected initial conditions in order to increase the confidence level.

Until now, we define how we select the constraint and initial value determination for the stability and

Presented at 45th European Rotorcraft Forum, Warsaw, Poland, 17-20 September, 2019

control derivatives which compose the state and control matrices (A_{phy}, B_{phy}). However, the T matrix whose elements are not physical do not have any constraints in our problem. Besides, considering Eq. (13), the initial value of T matrix is set to the inverse of the C matrix (obtained by subspace identification). This is not a compulsory practice; however a clever initialization of T that complies with the equations of the similarity transformation theory speeds up the computations. After setting up the constraints and the initial conditions, we continue with the optimization process. The *fmincon* solver of MATLAB is utilized as the optimization tool for our problem. The SQP algorithm is utilized here under a variety of initial conditions and constraints. The *fmincon* solver is externally assisted by the symbolic gradient of the objective function during the optimization process. This symbolic gradient is computed via the *gradient* command of MATLAB.

The optimization results are presented in Appendix (Fig. 3 and Fig. 4) Iteration index versus minimization output curves gathered from all of the optimization runs are presented here respectively for each stability and control derivatives. Each figure contains 50 optimization runs that are initiated for different initial values. Each figure is normalized by the true value of the associated derivative (in other words if optimization outputs converge to 1.0 this would mean that the estimation is perfect).The percent estimation errors for each parameter are tabulated Table 2. The formula for the calculation of the percent estimation error is given in Eq. (24).

$$estimation\ error\ (\%) = \left(\frac{estimated\ value - true\ value}{abs(true\ value)}\right) 100 \quad (24)$$

Another tool for the verification of the process is the comparison of time domain outputs of the true model and the estimated counterpart. For this purpose physical system matrices are constructed using the above presented optimization results. Then the true model and the estimated one are simulated with the same 3-2-1-1 excitation signals (Fig. 1). Afterwards, the Theil's inequality coefficient (TIC) is calculated using the two time domain outputs according to Eq.(25) [26] – [28].

$$TIC = \frac{\sqrt{\left({}^{1}/_{N}\right)\sum_{k=1}^{N}[z(t_k) - y(t_k)]^2}}{\sqrt{\left({}^{1}/_{N}\right)\sum_{k=1}^{N}[z(t_k)]^2} + \sqrt{\left({}^{1}/_{N}\right)\sum_{k=1}^{N}[y(t_k)]^2}} \quad (25)$$

As a rule of thumb, TIC values under 0.3 mean that the two models are complying [26]. In our case the TIC value is obtained as 0.21 verifying that the two models are highly complying and indicating that our estimation is quite accurate. The comparison of the true model outputs with the outputs of the model obtained through subspace identification and the outputs of the model obtained through physical subspace identification are shown Fig. 2.

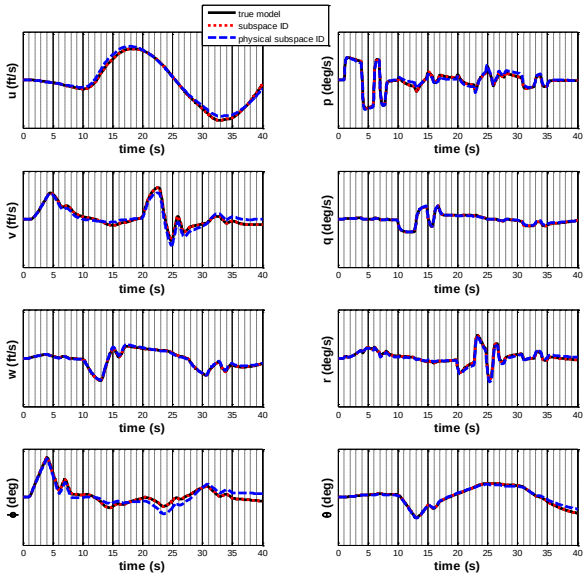

Fig. 2 Outputs for 3-2-1-1 Excitation Signals

In order to verify that our identification is still valid under different inputs, a doublet input is applied in four channels sequentially in another single test case. The inputs and the outputs of this test case are given in Fig. 5 and Fig. 6 respectively. The corresponding TIC value for this test case is 0.08.

8. CONCLUSION

This study presents implementation of physical subspace identification for a realistic helicopter. The unphysical system matrices are obtained by subspace identification and physical parameters are estimated by nonlinear constrained optimization. However this optimization problem may have infinitely many solutions if we do not define well-founded constraints. This study defines a methodology for constraint determination of the physical parameters. The results shows that it can be possible to find a solution if the constraints are assessed with physical meaning even though the error bound of all parameters are set to very large values (±50% for this problem).

Presented at 45th European Rotorcraft Forum, Warsaw, Poland, 17-20 September, 2019

References

[1] Van Overschee, P. and De Moor B., Subspace Identification for Linear Systems Theory - Implementation –Applications, Kluwer Academic Publishers, Boston/ London/ Dordrecht, 1996.

[2] Bittanti S., Lovera M., "Identification of Linear Models for a Hovering Helicopter Rotor", IFAC System Identitication, Kitakyushu, Fukuoka, Japan,1997.

[3] M. Verhaegen and A. Varga, "Some Experience with the MOESP Class of Subspace Model Identification Methods in identifying the BO105 Helicopter," tech. rep., German Aerospace Research Establishment, Institute for Robotics and System Dynamics, 1994.

[4] Lovera M., "Identification of MIMO State Space Models for Helicopter Dynamics", IFAC System Identitication, Rotterdam, Netherlands, 2003.

[5] I. Ping Li, " Subspace-based System Identification for Helicopter Dynamic Modelling", American Helicopter Society 63rd Annual Forum,Virginia Beach,VA, May 1-3, 2007.

[6] R.V., Flight Vehicle System Identification: A Time Domain Methodology, American Institute of Aeronautics and Astronautics Inc., Reston, VA, 2006

[7] Li, P., Postlethwaite, I., and Turner, M., "Subspace-Based System Identification for Helicopter Dynamic Modelling," American Helicopter Society 63rd Annual Forum Proceedings, Virginia Beach, VA, May 1–3, 2007.

[8] Wartmann J., Seher-Weiss S. "Application of the Predictor-Based Subspace Identification Method to Rotorcraft System Identification", 39th European Rotorcraft Forum, Moscow, Russia, 2013.

[9] Seher-Weiss S., "ACT/FHS System Identification Including Rotor and Engine Dynamics", AHS International 73rd Annual Forum & Technology Display, Fort Worth, Texas, USA, May 9–11, 2017.

[10] Li, P., Postlethwaite, I., "Subspace and Bootstrap-Based Techniques for Helicopter Model Identification", Journal of the American Helicopter Society, Vol. 56, 2011, DOI: 10.4050/JAHS.56.012002.

[11] Bergamasco, M. and Lovera, M., "Continuous-time predictor based subspace identification using Laguerre filters". IET Control Theory Applications, 5(7):856–867, 5 2011a.

[12] Bergamasco, M. and Lovera, M., Continuous-time predictor based subspace identification for helicopter dynamics. In 37th European Rotorcraft Forum, Gallarate, Italia, 2011b.

[13] Bergamasco, M. and Lovera, Rotorcraft system identification:an integrated time-frequency domain approach. In 2nd CEAS Specialist Conference on Guidance, Navigation & Control, Delft, The Nederlands, 2013.

[14] L. Liang Xie, L. Ljung, "Estimate Physical Parameters by Black-Box Modelling", In: Proc. 21st Chinese Control Conference. Hangzhou,China. pp. 673–677, 2002.

[15] Parrilo, P., Ljung, L., "Initialization of Physical Parameter Estimates", 13th IFAC Symposium on System Identification, Rotterdam, Netherlands, 3 December 2003.

[16] Lyzell, C., Enqvist, M., Ljung, L., "Handling Certain Structure Information in Subspace Identification", Proceedings of the 15th IFAC Symposium on System Identification Saint-Malo, France, July 6-8, 2009

[17] J. J. Ramos, Lopes dos Santos, P., "Mathematical Modeling, System Identification, and Controller Design of a Two Tank System", Proceedings of the 46th IEEE Conference on Decision and Control 46th IEEE Conference on Decision and Control New Orleans, LA, USA, Dec. 12-14, 2007

[18] J. Ramos, A., Mercére, G., Prot, O. "Parameter Estimation of Discrete and Continuous-Time Physical Models: A Similarity Transformation Approach", 49th IEEE Conference on Decision and Control, Atlanta, GA, USA, December 15-17, 2010.

[19] J. Ramos, Lopes dos Santos, P.," Identifying Second-Order Models of Mechanical Structures in Physical Coordinates: An Orthogonal Complement Approach", IEEE Europian Control Conference I, Zurih, Switzerland, July 17-19, 2013.

[20] S.Avcioglu, A.T. Kutay, K. Leblebicioglu.," Implementation of Physical Subspace Identification on a Realistic Helicopter, AIAA Science and Technology Forum and Exposition 2019, San Diego, CA,USA, January 7-12,2019.

[21] Hespanha, J. P, Linear System Theory, Princeton University Press, 2009, Chap. 13.

[22] Padfield, Gareth, "Helicopter Flight Dynamics: The Theory and Application of Flying Qualities and Simulation Modeling, American Institute of Aeronautics and Astronautics", Washington D.C., 1996.

[23] Nocedal, J. and S. J. Wright. Numerical Optimization, Second Edition. Springer Series in Operations Research, Springer Verlag, 2006.

[24] Benson, H. Y., D. F. Shanno, and R. J. Vanderbei, "A Comparative Study of Large-Scale Nonlinear Optimization Algorithms" in High Performance Algorithms and Software for Nonlinear Optimization, G. Di Pill0 and A. Murli (Eds.), Kluwer Academic, Nonvell, MA, pp. 95-128, 2003.

[25] Tischler, M. B. and Remple, R. K., "Aircraft and Rotorcraft System Identification: Engineering Methods with Flight-Test Examples", American Institute of Aeronautics and Astronautics, Inc., Reston, VA, 2nd edition, 2012.

[26] Jategaonkar, R.V., "Flight Vehicle System Identification: A Time Domain Methodology", American Institute of Aeronautics and Astronautics Inc., Reston, VA, 2006.

[27] Murray-Smith, D. J, "Methods for the External Validation of Continuous System Simulation Models: A Review," Journal of Mathematical Modelling of Systems, Vol. 4, No., pp. 5–31, 1998.

[28] Fischenberg, D., Jategaonkar, R., von Gruenhagen, W., "Aerodynamic Modeling and System Identification from Flight Data—Recent Applications at DLR," Journal of Aircraft, Vol. 41, No. 4, pp. 681–691, 2004.

Presented at 45th European Rotorcraft Forum, Warsaw, Poland, 17-20 September, 2019

Appendix

$$A_{phy} = \begin{bmatrix} X_u & X_v & X_w & X_p & X_q - w_0 & X_r + v_0 & 0 & -gcos\theta_0 \\ Y_u & Y_v & Y_w & Y_p + w_0 & Y_q & Y_r - u_0 & gcos\phi_0 cos\theta_0 & -gsin\phi_0 sin\theta_0 \\ Z_u & Z_v & Z_w & Z_p - v_0 & Z_q + u_0 & Z_r & -gsin\phi_0 cos\theta_0 & -gcos\phi_0 sin\theta_0 \\ L_u & L_v & L_w & L_p & L_q & L_r & 0 & 0 \\ M_u & M_v & M_w & M_p & M_q & M_r & 0 & 0 \\ N_u & N_v & N_w & N_p & N_q & N_r & 0 & 0 \\ 0 & 0 & 0 & 1 & sin\phi_0 tan\theta_0 & cos\phi_0 tan\theta_0 & 0 & 0 \\ 0 & 0 & 0 & 0 & cos\theta_0 & -sin\theta_0 & 0 & 0 \end{bmatrix}$$

$$B_{phy} = \begin{bmatrix} X_{lat} & X_{lon} & X_{ped} & X_{col} \\ Y_{lat} & Y_{lon} & Y_{ped} & Y_{col} \\ Z_{lat} & Z_{lon} & Z_{ped} & Z_{col} \\ L_{lat} & L_{lon} & L_{ped} & L_{col} \\ M_{lat} & M_{lon} & L_{ped} & M_{col} \\ N_{lat} & N_{lon} & N_{ped} & N_{col} \\ 0 & 0 & 0 & 0 \\ 0 & 0 & 0 & 0 \end{bmatrix}$$

Presented at 45th European Rotorcraft Forum, Warsaw, Poland, 17-20 September, 2019

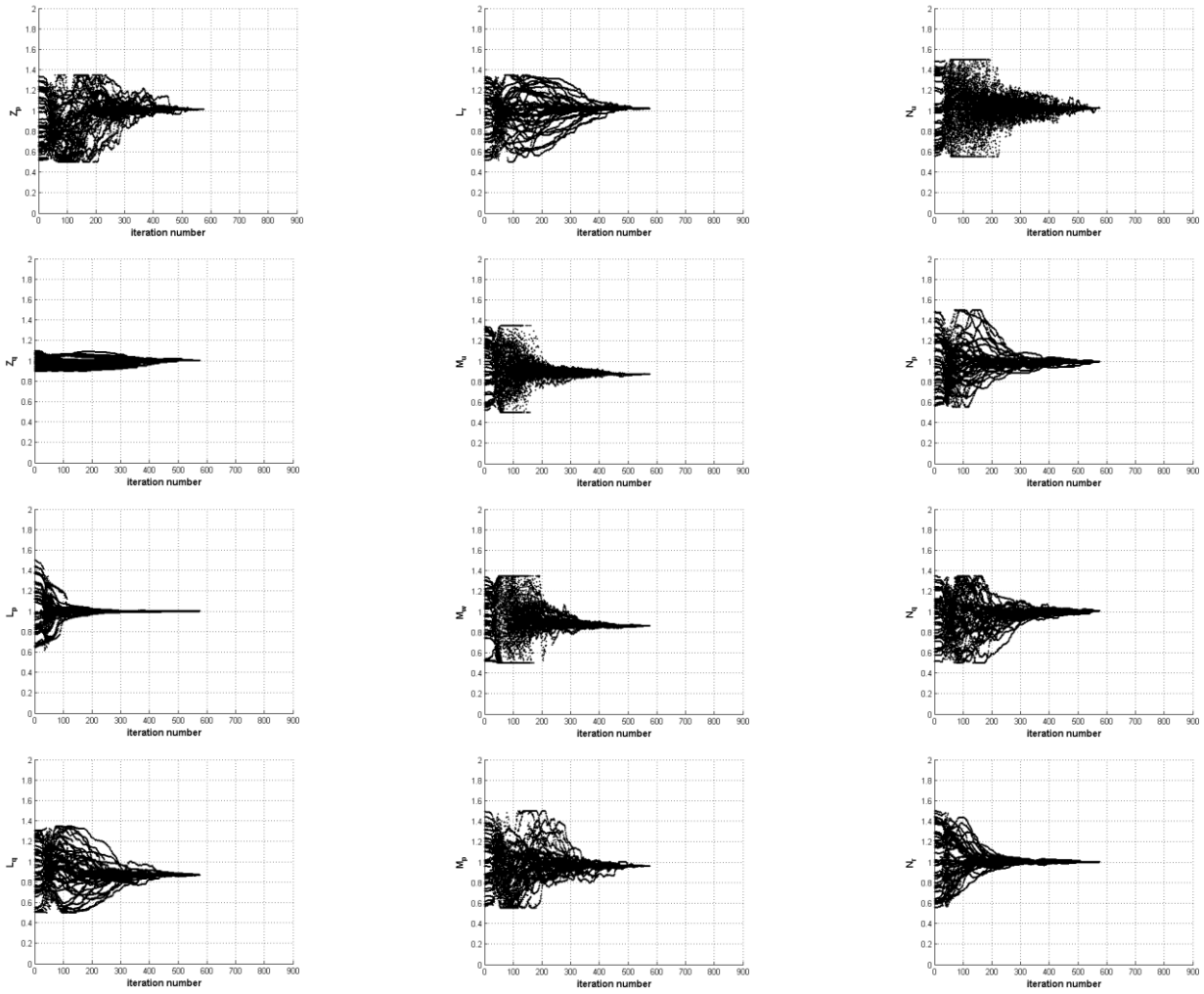

Fig. 3 Convergence of Stability Derivatives

Presented at 45th European Rotorcraft Forum, Warsaw, Poland, 17-20 September, 2019

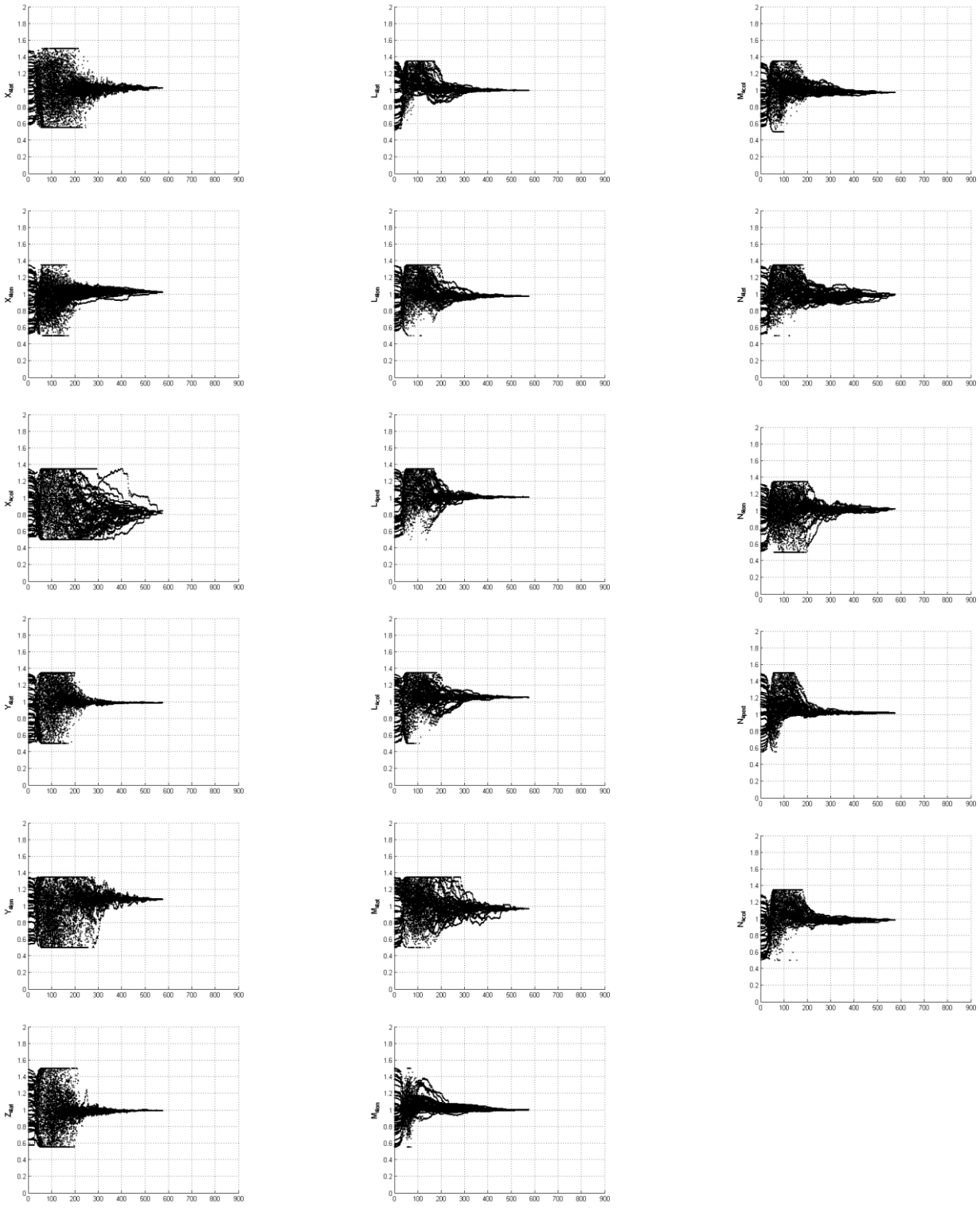

Fig. 4 Convergence of Control Derivatives

Presented at 45th European Rotorcraft Forum, Warsaw, Poland, 17-20 September, 2019

Table 2 Estimation Errors of Stability & Control Derivatives

parameter	symbol	units	error bound (lower). %	estimation error. %	error bound (upper). %	parameter	symbol	units	error bound (lower). %	estimation error. %	error bound (upper). %
x_1	X_u	1/s	-50	6.632	50	x_{31}	N_u	rad/(ft.s)	-50	-2.510	50
x_2	X_v	1/s	NA	NA	NA	x_{32}	N_v	rad/(ft.s)	-50	6.457	50
x_3	X_w	1/s	NA	NA	NA	x_{33}	N_w	rad/(ft.s)	NA	NA	NA
x_4	X_p	ft/(rad.s)	-50	19.656	50	x_{34}	N_p	1/s	-50	0.973	50
x_5	X_q	ft/(rad.s)	-50	-30.539	50	x_{35}	N_q	1/s	-50	-0.184	50
x_6	X_r	ft/(rad.s)	-50	8.928	50	x_{36}	N_r	1/s	-50	-0.081	50
x_7	Y_u	1/s	NA	NA	NA	x_{37}	$X_{\delta lat}$	ft/(s^2%)	-50	-2.400	50
x_8	Y_v	1/s	-50	-3.494	50	x_{38}	$X_{\delta lon}$	ft/(s^2%)	-50	-2.403	50
x_9	Y_w	1/s	NA	NA	NA	x_{39}	$X_{\delta ped}$	ft/(s^2%)	NA	NA	NA
x_{10}	Y_p	ft/(rad.s)	-50	6.476	50	x_{40}	$X_{\delta col}$	ft/(s^2%)	-50	16.211	50
x_{11}	Y_q	ft/(rad.s)	-50	-33.843	50	x_{41}	$Y_{\delta lat}$	ft/(s^2%)	-50	1.204	50
x_{12}	Y_r	ft/(rad.s)	-50	-0.121	50	x_{42}	$Y_{\delta lon}$	ft/(s^2%)	-50	-8.352	50
x_{13}	Z_u	1/s	NA	NA	NA	x_{43}	$Y_{\delta ped}$	ft/(s^2%)	NA	NA	NA
x_{14}	Z_v	1/s	NA	NA	NA	x_{44}	$Y_{\delta col}$	ft/(s^2%)	NA	NA	NA
x_{15}	Z_w	1/s	NA	NA	NA	x_{45}	$Z_{\delta lat}$	ft/(s^2%)	-50	0.878	50
x_{16}	Z_p	ft/(rad.s)	-50	-1.353	50	x_{46}	$Z_{\delta lon}$	ft/(s^2%)	-50	0.000	50
x_{17}	Z_q	ft/(rad.s)	-50	-0.293	50	x_{47}	$Z_{\delta ped}$	ft/(s^2%)	-50	50.000	50
x_{18}	Z_r	ft/(rad.s)	-50	-29.886	50	x_{48}	$Z_{\delta col}$	ft/(s^2%)	-50	0.000	50
x_{19}	L_u	rad/(ft.s)	-50	-5.804	50	x_{49}	$L_{\delta lat}$	rad/(s^2%)	-50	0.100	50
x_{20}	L_v	rad/(ft.s)	-50	-13.056	50	x_{50}	$L_{\delta lon}$	rad/(s^2%)	-50	2.532	50
x_{21}	L_w	rad/(ft.s)	-50	44.509	50	x_{51}	$L_{\delta ped}$	rad/(s^2%)	-50	-1.100	50
x_{22}	L_p	1/s	-50	0.022	50	x_{52}	$L_{\delta col}$	rad/(s^2%)	-50	-5.346	50
x_{23}	L_q	1/s	-50	12.606	50	x_{53}	$M_{\delta lat}$	rad/(s^2%)	-50	3.360	50
x_{24}	L_r	1/s	-50	-2.390	50	x_{54}	$M_{\delta lon}$	rad/(s^2%)	-50	-0.032	50
x_{25}	M_u	rad/(ft.s)	-50	12.714	50	x_{55}	$M_{\delta ped}$	rad/(s^2%)	NA	NA	NA
x_{26}	M_v	rad/(ft.s)	NA	NA	NA	x_{56}	$M_{\delta col}$	rad/(s^2%)	-50	2.756	50
x_{27}	M_w	rad/(ft.s)	-50	13.706	50	x_{57}	$N_{\delta lat}$	rad/(s^2%)	-50	1.529	50
x_{28}	M_p	1/s	-50	3.964	50	x_{58}	$N_{\delta lon}$	rad/(s^2%)	-50	-1.579	50
x_{29}	M_q	1/s	-50	-0.039	50	x_{59}	$N_{\delta ped}$	rad/(s^2%)	-50	-1.811	50
x_{30}	M_r	1/s	NA	NA	NA	x_{60}	$N_{\delta col}$	rad/(s^2%)	-50	1.641	50

Presented at 45th European Rotorcraft Forum, Warsaw, Poland, 17-20 September, 2019

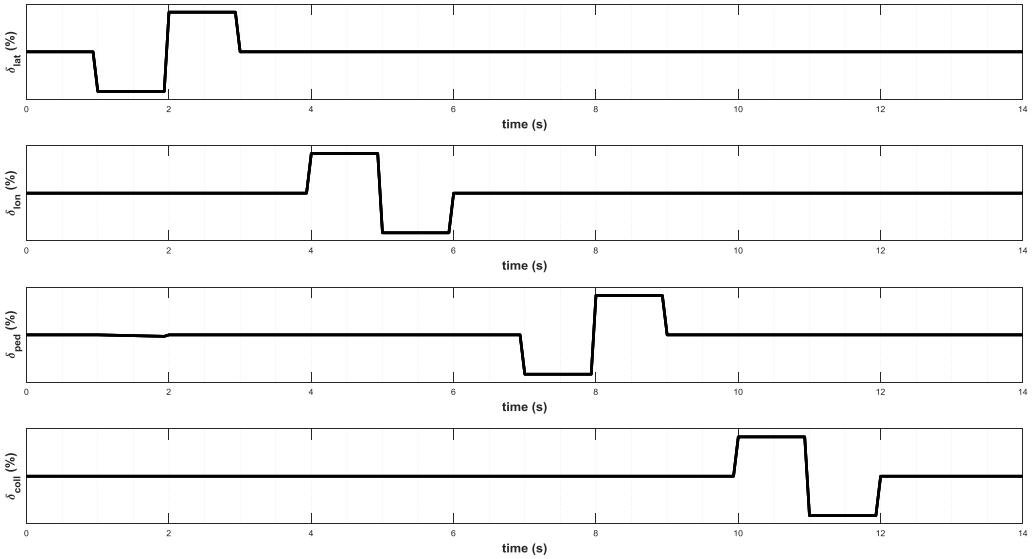

Fig. 5 Input Signals (Doublet)

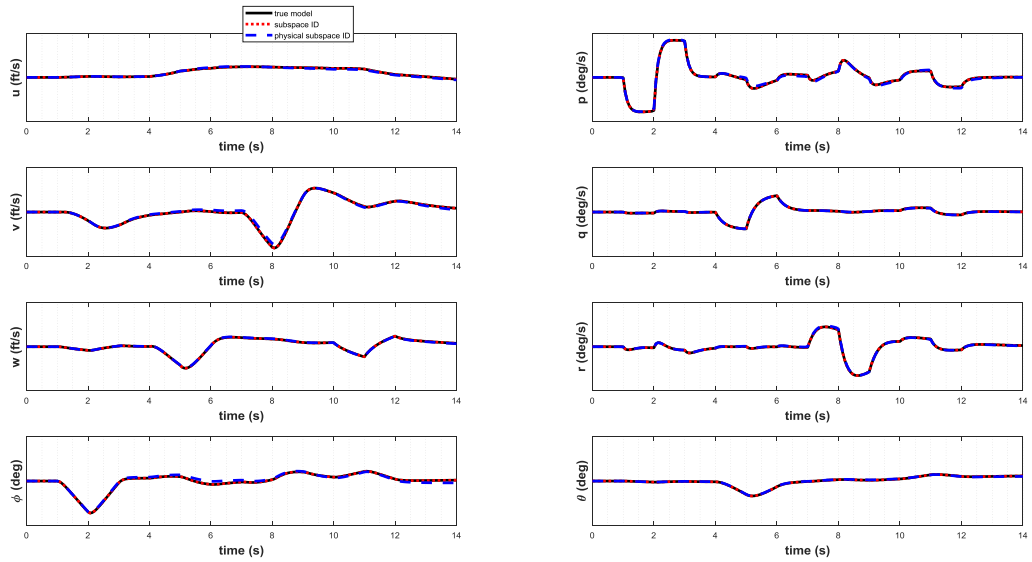

Fig. 6 Comparison of Outputs for Doublet Excitation Signals

Presented at 45th European Rotorcraft Forum, Warsaw, Poland, 17-20 September, 2019